RADIO-FREQUENCY SIZE EFFECT IN INDIUM

V. F. GANTMAKHER and I. P. KRYLOV

Institute of Solid State Physics and Institute for Physics Problems, Academy of Sciences, U.S.S.R.

Submitted to JETP editor May 21, 1965

J. Exptl. Theoret. Phys. (U.S.S.R.) **49**, 1054–1067 (October, 1965)

The Fermi surface of indium is investigated by means of the rf size effect at 3 Mc/sec. For identification of the observed cross sections extensive use is made of the dependence of the size effect lines on the inclination of the magnetic field relative to the sample surface. The complex shape of the equal-energy surface in the second zone leads to the appearance of several size effect lines due to sharp bends in electron trajectories within a magnetic field. These lines are not associated with the electromagnetic field spikes inside the metal but to less pronounced characteristics of the field between the spikes. The entire set of lines pertaining to the second zone Fermi surface confirms the close similarity of this surface to the nearly free electron model. No lines were observed that would indicate openness of the Fermi surface. It also follows from the experimental data that the third zone Fermi surface consists of tubes that have their axes along $\langle 110 \rangle$ and that are joined to form rings. The form of the central cross section of a tube produced by an intersection with a plane perpendicular to its axis was determined by using several samples with different directions of the normals. No lines were observed that would indicate the existence of tubes with axes parallel to $\langle 101 \rangle$.

ALTHOUGH experimental methods for studying the energy spectra of electrons have been intensely developed during recent years, the Fermi surfaces of many transition metals are known only in a general way. For the development of the corresponding theory it is important to know the properties and exact forms of the Fermi surfaces near selected directions in the reciprocal lattice. This is of some special importance for metals with distorted crystal structure. Abrikosov and Fal'kovskiĭ[1] have shown that in Bi-type metals the structural distortion can be accounted for by the electronic part of the binding energy. This is probably true also for several other metals including indium. Let us consider indium and aluminum, which are in the same column of the periodic table, having three valence electrons. Their crystal structures differ only slightly; the tetragonal lattice of In is obtained by 8% stretching of the Al cubic lattice along one of the C_4 axes.

It can be seen even from the (almost) free-electron model that this relatively small deformation can induce important changes in the energy spectrum; the hole surface in the second zone reaches the corners of the zone and tends to become an open surface (Fig. 1). It is therefore of interest to make a careful comparison between the Fermi surfaces of these two metals.

The Fermi surface of Al is now relatively well understood as a result of many experimental investigations, the latest and most thorough of which are the measurements of Kamm and Bohm (magneto-acoustic oscillations),[2] and of Vol'skiĭ (quantum oscillations of the surface impedance).[3] In the case of In, which has been studied less thoroughly, we have the following information. The galvano-magnetic measurements in[4,5] show that there are
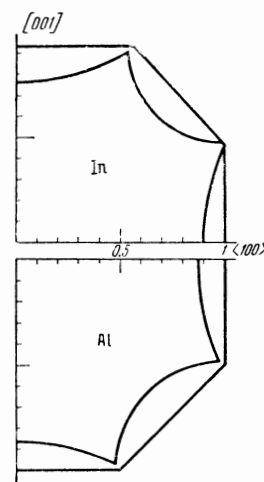
FIG. 1. Intersections of the second zone Fermi surfaces of Al and In with a (010) plane in the almost free electron approximation.

no open trajectories in indium. Rayne's study of ultrasonic absorption[6] has qualitatively confirmed the existence of a large hole surface in the second zone, which was predicted by the free-electron model. Mina and Khaĭkin[7] recently investigated this surface more thoroughly by means of cyclotron resonances and their cutoff fields. The measurements of the de Haas—van Alphen oscillations in[8,9] indicate the existence of tubes along the edges of the Brillouin zone; however, the existence of tubes in (100) planes (α tubes) was not confirmed in[7]. Some information concerning the behavior of the Fermi surface at the corners of the Brillouin zones is given in[8] [the angular dependences of long-period oscillations in the (001) and (100) planes within a magnetic field].

We have studied the electronic structure of In using an additional independent method, the rf size effect,[10,11] and present our results in the present article.

EXPERIMENT

Our experimental work consisted in measuring the surface impedance $Z = R + iX$ of monocrystalline In plates as a function of the magnetic field **H**. It is known that for values of H at which the characteristic dimension of the extremal electron trajectory equals the thickness d of a plate singularities appear in the function Z(H). By registering these singularities we can determine the corresponding dimension 2p of the electron orbit in momentum space, using the formula

$$2p = ec^{-1}dH. \tag{1}$$

The technique used to observe the rf size effect was described in[10]. Improved apparatus was used in the experimental work on In, permitting measurements of both the oscillator frequencies $f(\partial f/\partial H \sim -\partial X/\partial H)$ and their amplitudes $u(\partial d/\partial H \sim -\partial R/\partial H)$. For this purpose some elements of the measuring circuit described in[10] were replaced by an amplitude modulation detector and the measurement generator was operated close to threshold. The results obtained by the two methods have been compared in[12]. The frequency used in our experiments was close to 3 Mc/sec and the modulation frequency was 20 cps.

The error ($\sim 7\%$) of absolute pulse measurements resulted from an error (2—3%) in measuring the thickness of the sample and from uncertainty (up to 5%) in selecting the reference field strength within the line width. For size effect lines, whose shape does not vary within the entire angular interval where they exist, relative changes
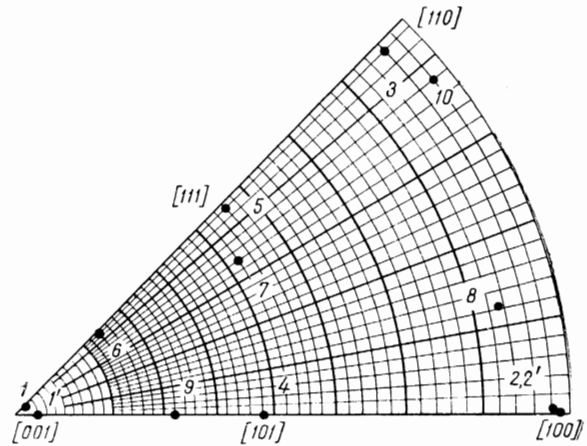

FIG. 2. Directions of normals to the plane surfaces of samples in stereographic projection.

in the dimensions of extremal cross sections of the Fermi surface are determined with considerably higher accuracy ($\sim 0.5\%$).

The angular dependences of the positions of the size effect lines were investigated in 12 samples, which were disks 18 mm in diameter that had been grown from a melt in a demountable quartz form. Figure 2 shows the orientations of their normals **n** determined by means of x-rays. The single-crystal character of all samples was tested by etch fig-
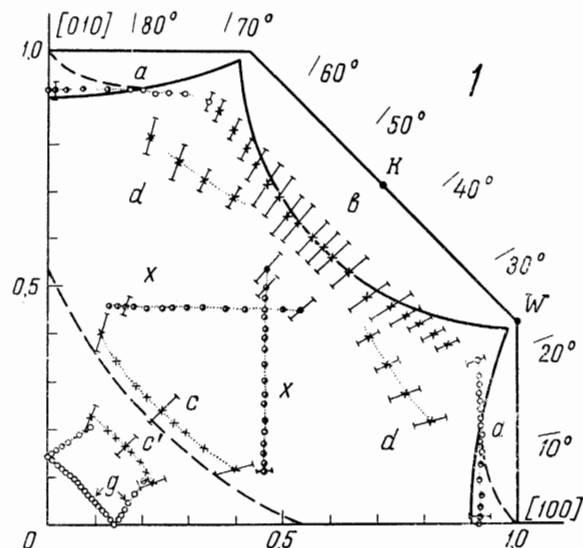

FIG. 3. Anisotropy of extremal orbit dimensions in the (001) plane — diagram 1. Solids lines — cross sections of the Brillouin zone and of the Fermi surface on the free-electron model. Dashed lines — projection of the Fermi surface contour. × — strongest lines; the remaining symbols indicate the character of the dependence on magnetic field inclination: o — absence of inclination effect, ◑ — splitting, ● — line shift (see the following diagrams), □ — complex dependence accompanied by a change of line shape (see the following diagrams).
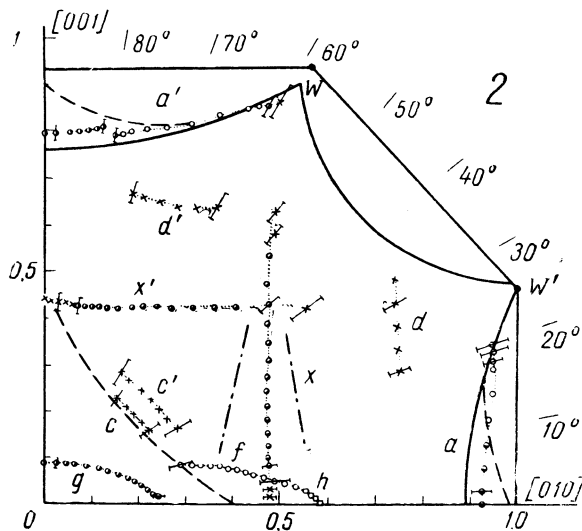
FIG. 4. Data for the (100) plane — diagram 2, with the same notation as in diagram 1. Dot-dash line — location of the x cross sections for sample 8 (the projection of the [010] direction on the plane of the sample is along the abscissa axis).

FIG. 6. Data for the (011) plane — diagram 4, with the same notation as in diagram 1. Dot-dash lines — locations of the y cross sections for sample 9 (the direction of the [100] axis coincides with the direction indicated in the diagram).

ures, because it was found in the course of the experiments that in some directions of growth two or three crystals often grow instead of one with different orientations forming an angle of about 90°. Neither the intensity nor width of any line was affected by the etching process. The thickness d was 0.40 mm for samples 1', 2', and 8; 0.29 mm for samples 1 and 3; 0.30 mm for all other samples.

The most thoroughly investigated samples had normals close to the rational crystallographic directions. The results are shown in the polar diagrams 1—5 (Figs. 3—7). Values of p obtained

from Eq. (1) are plotted radially in the n × H direction. All quantities are given in units of $p_0 = 2\pi\hbar/a = 1.455 \times 10^{-19}$ g-cm/sec, where p_0 is the boundary momentum of the Brillouin zone in the [100] direction, and a is the lattice constant at helium temperatures.

All values of p in the angular diagrams were obtained with a magnetic field H parallel to the sample surface. However, in identifying the cross sections we used extensively the dependence of line position on the inclination (tip) of the magnetic field.[11] We determined this dependence for all fairly intense lines in the range of inclinations from 0° to + 4°. In the diagrams the inclination-dependent
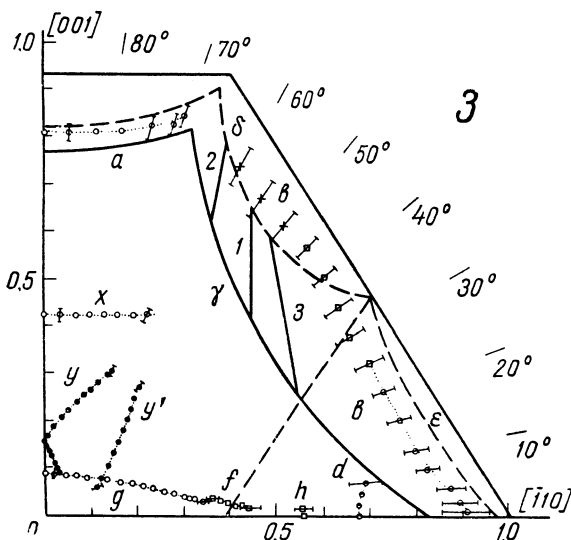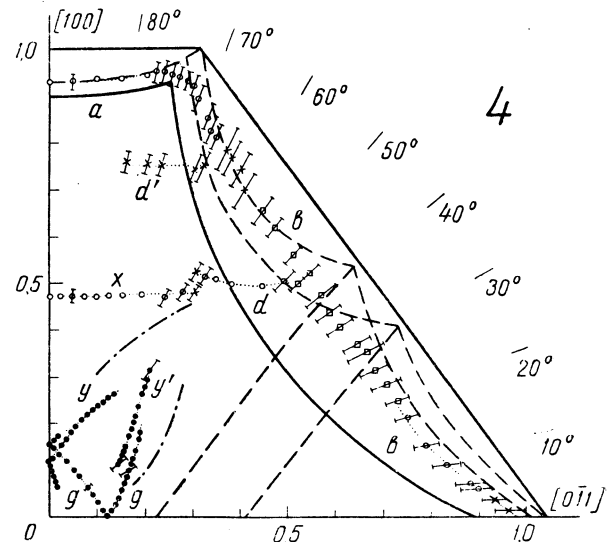
FIG. 5. Data for the (110) plane — diagram 3, with the same notation as in diagram 1. The segments 1, 2, and 3 are explained in the text.
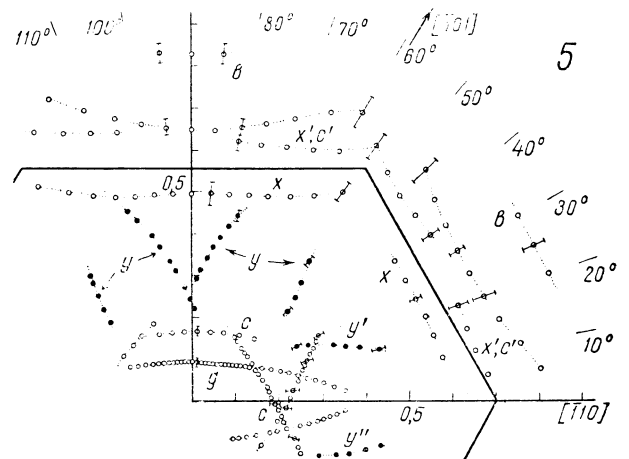
FIG. 7. Data for the (111) plane — diagram 5, with the same notation as in diagram 1. Solid line — hexagonal face of the Brillouin zone.
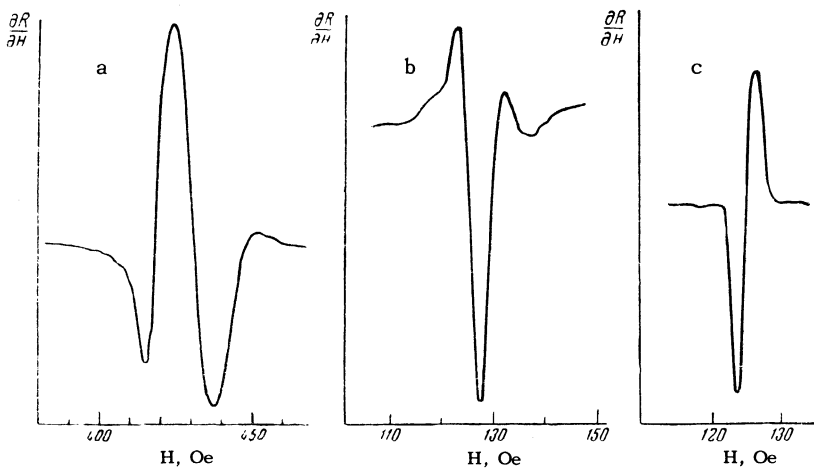
FIG. 8. Different types of size effect lines in indium. a — line a_2 in sample 2' with $H \parallel [001]$ and polarization $E_\sim \parallel [010]$; b — line g in sample 1 with H at 20° to [100] and $E_\sim \parallel [010]$; c — line y' in sample 3 with H at 40° to [001] and $E_\sim [\bar{1}10]$.

behavior of the lines is designated by different symbols (see the legend of Fig. 3).

The errors indicated in the polar diagrams resulted only from the line width. For lines whose shapes do not vary with the field direction, the errors are indicated only near the ends of the angular interval.

All the strongest principal line groups have characteristic shapes that are very similar on the different crystallographic planes. Figure 8 shows traces of a, g, and y lines; the x lines have the same shape as the y lines.

Observation of the size effect requires a long mean free electron path and therefore a low temperature T. In indium the latter requirement is intensified by its low Debye temperature, which results in a strong temperature dependence of the line amplitude even at helium temperatures. For example, when the temperature was reduced from 3° to 1.3°K the intensity of line group a_1 in sample 1' increased by a factor of more than 30. (The diagrams will henceforth be designated by appropriate indices; for example, a_1 designates a line of the group a in a sample with $n \parallel [001]$.) At T = 1.3°K the mean free path evaluated from the amplitudes of size effect lines for helical trajectories was 0.5 mm.[11] It should be noted that, because of the superconducting transition of In the low-field region had to be investigated at higher temperatures, thus making the experimental work much more difficult.

Lines resulting from chains of orbits[13] are not shown in the diagrams. However, lines of a + g chains were observed on all planes, in addition to the a lines. In a doubled field the lines were usually 5—10 times weaker, with the exception of the x_2 line, which was weakened by a factor of only 1.5—2.

THE FERMI SURFACE IN THE THIRD ZONE

Our identification of the cross sections will begin with the third zone. According to the free-electron model, the constant-energy surface in this zone should consist of tubes along the edges of the Brillouin zone.[8] It is easily seen that all g cross sections pertain to tubes in the (001) plane (β tubes). This is indicated by the dependence of the lines on the field inclination, as well as by the dimensions and shapes of the cross sections. The absence of dependence on the inclination in the case of the g_1, g_3, and g_5 lines is accounted for by the fact that the β tubes in these cases lie in the plane of the sample; the g_4 lines are seen on tubes having their axes inclined 31° to the plane of the sample; finally, the splitting of the g_2 lines is accounted for by the presence of two symmetrically inclined β tubes.

The existence of f and h lines and their anisotropy is easily explained if it is assumed that the β tubes are joined to form "rings" as for Al. Then f_2 is determined by an orbit passing through two tubes (Fig. 9), f_3 by an orbit passing through three tubes, and h_2 and h_3 by an orbit along the outside contour of the ring. The angular intervals within which these cross sections exist and the dimensions that they determine provide convincing support for this interpretation, although we do not completely understand the inclination dependence of the f_3 and h lines (strong effects may possibly be caused here by small deviations of the normal to the sample surface from a rational crystallographic direction). The existence of a ring is indicated by the fact that the g_1 line is visible in a relatively small angular interval (~ 72°); at large angles the cross section goes to a saddle point inside the ring. It must also be mentioned that we
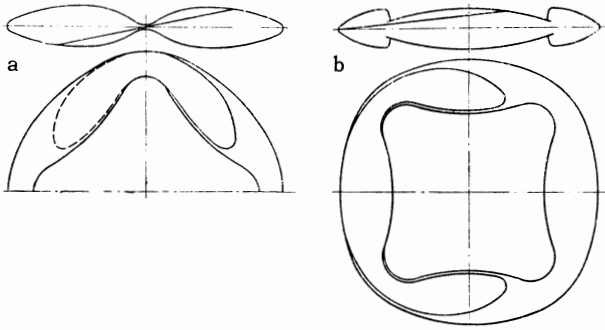
FIG. 9. Schematic drawing of f orbits — profile (from the direction of the normal n), and plane of the ring. $a - f_2$ orbits, $n \parallel [100]$; $b - f_3$ orbits, $n \parallel [110]$.

FIG. 10. Central cross section of the β tube in the (110) plane based on experimental data.

were unable to detect orbits similar to h inside the ring.

Our results confirm the conclusions of Mina and Khaĭkin[7] regarding the existence of a β-tube ring. A serious discrepancy in the observed ranges of lines between our work and[7] occurs only in the (001) plane; in[7] cyclotron resonance is seen at 83°. A probable explanation is that cross sections with extremal dimensions and with extremal effective masses differ in the present case because there is no central symmetry.

It is difficult to determine the exact shape of the tube from the g cross sections if the tube is not axially symmetric. Therefore, for example, the extremal g_1 cross sections are shifted slightly with respect to the point K at the middle of the corresponding Brillouin zone edge (Fig. 3). However, if the magnetic field is along the [110] direction, the extremal intersections of the tube with the (110) plane must pass through K. We obtained four different dimensions of this cross section from samples 1, 6, 5, and 3. We must also take into account the existence of a symmetry plane for this cross section (represented by the line AB in Fig. 10) and also the cross-sectional area known from[8]. There is little arbitrariness involved in plotting a cross section satisfying all these conditions. For example, the point C cannot be shifted to the right because of the dimension at 66°, while a shift to the left retaining all linear dimensions leads to an increase of the area. The situation of the plotted cross section with respect to the point K should in principle be determined by the h_3 line. However, since the dimension of h_3 is large, the absolute error becomes too large. Therefore the distance BK in Fig. 10 cannot be determined from our experiments and has been selected arbitrarily.

We did not directly observe extremal cross sections on the necks between tubes. From the angular interval for the existence of the h_3 line we
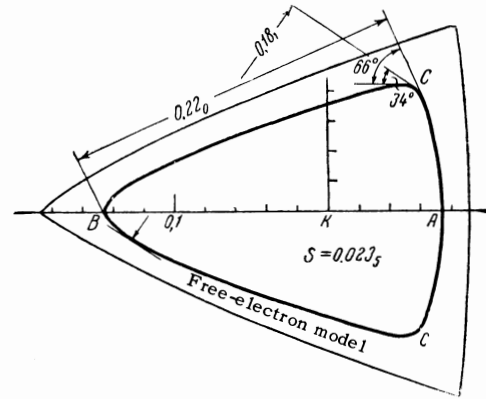
obtain 0.03 as the dimension of the neck in the [001] direction. In the [100] direction a dimension of the order of 0.1 is obtained from the g_1 cross section at the boundary of its existence interval.

With regard to the existence of α tubes, we decide immediately that these are not related to the y lines. Firstly, the y lines go into the region of dimensions exceeding the maximum possible α-tube length. Secondly, in low fields the y cross sections are separated and do pass into each other continuously. The region of discontinuity is found in field directions close to the axis of the postulated tube. One might imagine that α tubes are connected in sets of four at the W′ corners of the reciprocal lattice (Fig. 4). However, this cruciform surface evidently could not give the observed dependence of y lines on the field inclination. We note that in the case of a tube inclined to the metal surface with the field passing through a plane perpendicular to the tube axis, the line shift as a linear function of the inclination should exhibit a reversal of sign. This is actually observed for a β tube in diagram 4; the two g_4 branches have different signs for the linear shift. On the other hand, for the y lines the sign of the shift does not change upon passing from one branch to the other. Finally, as can be seen from diagram 5, the y lines are quite symmetrically located and the $\langle 110 \rangle$ and $\langle 101 \rangle$ directions do not differ qualitatively; the α tubes alone, without β tubes, do not possess this symmetry.

The joining of α tubes to β tubes at the corners W is excluded by the fact that the g_3 and g_5 cross sections are visible in a large angular interval, the f_2 cross sections pass continuously into h_2, and also because of the features of the effective mass changes noted in[7].

We also note that if the α-tube dimensions were of the order of 0.05, so that it would be difficult to

use them for direct observation of the size effect, their existence could still be observed from the $a_2 + \alpha$ and $a_4 + \alpha$ chains.

Therefore, while cross sections of β tubes were visible in samples of all orientations, with no orientation did we observe lines that could be interpreted as α-tube sections. The situation is similar in connection with the observation of cyclotron resonance in[7], but conflicts with the data given in the latest work on the de Haas—van Alphen effect.[9] We therefore attempted to reproduce the results of Brandt and Rayne,[8,9] employing the quantum oscillations of the surface impedance[3] in fields up to 11 kOe. Oscillations corresponding to β tubes were observed with a sensitivity margin of two to three orders of magnitude, but neither long-period oscillations nor α-tube oscillations were visible.

The cause of this disagreement with the aforementioned authors is not clear. It is unlikely that we used insufficiently high fields.

Conclusion. The foregoing discussion shows that all high-frequency measurements (cyclotron resonance and the size effect) indicate that the third zone contains only β tubes that are connected to form rings.

THE FERMI SURFACE IN THE SECOND ZONE

We shall now proceed to discuss the hole surface in the second zone, containing primarily a group of a lines, which are the most intense of all those observed in indium. These lines determine the distance between opposite square "cups" of the surface (Fig. 11). The dependence of these lines on the inclination has been thoroughly discussed in[11]. This dependence alone provides proof that the form of the surface is very close to the free-electron model.
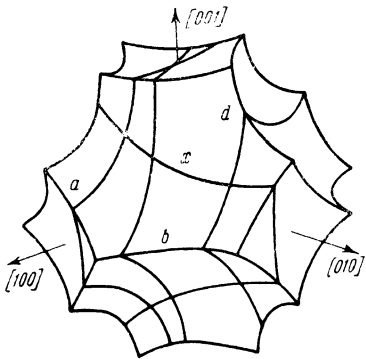
Much weaker b lines are observed when the trajectory enters the skin layer at a small angle. In the corresponding field directions the trajectory dimension in most cases varies nonmonotonically as a function of p_H, so that there is no very clear extremal cross section. This probably accounts in some instances for the complex inclination independence of lines, accompanied by a change of their shape.

The d lines are evidently determined by different extremal cross sections far from the central cross sections, appearing because of the corners of the Fermi surface. For example, the d_3 line results from an orbit passing through the corners of four square cups. The d_1 orbit is shown in Fig. 11.

It is well known that in the case of a complicated electron trajectory the periods of magneto-acoustic oscillations are determined by the width of only a part of the trajectory.[14] Then the condition $\mathbf{v} \cdot \mathbf{q} = 0$ (where $\mathbf{v}$ is the electron velocity and $\mathbf{q}$ is the sound wave vector) must be fulfilled at more than two points of the trajectory. For the size effect analogous points are given by the condition

$$\mathbf{vn} = 0 \qquad (2)$$

in conjunction with the additional requirement that the portion of the trajectory between two such points lie entirely in the region between the tangents to the trajectory at the given points. We observed size effect lines of this kind experimentally. Figure 12 elucidates the origin of lines c and c'. It is easily verified that twice the dimension of c' added to the dimension of c gives the dimension of b.

The lines c_1 and c_2 are weaker by a factor of 100 than the a lines. The x lines in diagrams 1—4 are much more intense. It is easily seen that these lines determine a dimension that is exactly half of the a dimension. We assume that the appearance of these lines is associated with the existence of
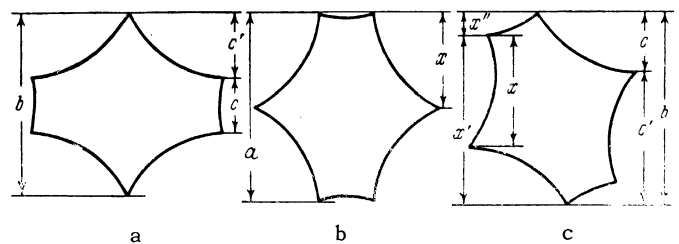
FIG. 11. Second zone Fermi surface of In on the free-electron model. Different orbits are shown for a sample with $\mathbf{n} \parallel [001]$.

FIG. 12. Measured central cross section dimensions of the second zone Fermi surface for different normals n with a fixed field direction $\mathbf{H} \parallel [011]$. a — sample 2, diagram 2 (line b was not observed experimentally); b — sample, 4, diagram 4; c — sample 7 (line x″ was not observed).

sharp bends of the electron trajectories (Fig. 12b). This explanation postulates the existence of an alternating electromagnetic field not only near the "spikes,"[15,13,16] at depths determined by the locations on the trajectories of points for which (2) is fulfilled; this field, although it is weaker than near the spikes, should exist between the latter.

In order to show this quantitatively, let us consider the distribution of the electromagnetic field inside the metal if it has a Fermi surface in the form of a circular cylinder parallel to the metal surface. An electron receives a velocity increase Δv in a skin layer of thickness δ and as the carrier of the current $\Delta j = e \Delta v$ penetrates inside along a circular trajectory. If at a depth z its motion is in a direction making the angle φ with the surface, then the horizontal component of the generated current is $e \Delta v \cos \varphi$. (The vertical component is compensated by electrons moving along the same trajectory at the angle $\varphi_1 = 2\pi - \varphi$ with respect to the surface.) Assuming that the number of electrons belonging to the given trajectory at the depth z is proportional to $1/\sin \varphi$, we find[15] that for $z \gg \delta$ and $2r - z \gg \delta$ (i.e., far from the spikes) the current generated by these electrons is

$$j(z) \approx j(0) \sqrt{\delta / r} \cot \varphi \qquad (3)$$

where r is the radius of the electron trajectory. We thus see directly that with a more complex trajectory the existence of a bend, i.e., the jump of φ, leads to a jump of j(z). The emergence of this jump on the opposite surface causes the appearance of size effect lines.

The x lines are about 10 times weaker than the a lines, corresponding to $\sqrt{\delta/r}$ in order of magnitude. The angular intervals of the x lines coincide with the intervals in which there exist orbits passing through square cups and edges between two hexagonal cups. The corresponding electron trajectories in coordinate space have segments parallel to the surface and a sharp bend. In diagrams 1 and 2 as the field approaches the directions [001] and $\langle 100 \rangle$ these trajectories disappear (Fig. 11); the x lines then disappear also.

We believe that the foregoing is the only possible way to account for the x lines. No explanations involving specular reflections are acceptable, because the effect is not modified by etching of the sample. Magnetic breakdown or open trajectories would indicate a dimension associated with the reciprocal lattice (for example, 0.5 in diagram 1) rather than with the dimension of the surface in the second zone. In principle quantum effects could exist at sharp bends of quasi-classical orbits, but

we do not think that the foregoing experiments support any such hypothesis.

The corners of the Fermi surface should be rounded, as a general rule. Since the x lines are not wider than the a lines, it follows that the ratio of the rounding radius to the total orbital dimension is smaller than the relative line width $\Delta H/H \sim 3\%$. This agrees qualitatively with the calculations of Segall for Al in[17], which contains a figure where the radius of rounding of the edges between two hexagonal cups is very much smaller than the radius of rounding of the other edges.

If we take samples with different directions of the normal **n** and a fixed direction of the field **H** with respect to the crystallographic axes, the trajectories will be rotated differently with respect to the surface of the sample. In Fig. 12 this field direction is along [011]. It is easily seen that as the normal to the surface is rotated in the (011) plane the x lines become c lines and vice versa. Therefore for samples of intermediate orientations (as in diagram 5) the distribution of the lines in the x and c groups is very arbitrary.

In diagram 5, in the direction $\sim 30°$ (perpendicular to $\langle 011 \rangle$) three cross sections are clearly seen with dimensions that coincide with the corresponding dimensions of the x and c lines. It must be remembered that for **n** ‖ [111] the dimensions of c and x″, and therefore of c′ and x′, are very similar (Fig. 13). Diagram 5 shows that as the field is rotated one of these paired cross sections is split. Four out of the five x and c dimensions are seen in sample 7; the lowest dimension (x″) does not appear in this sample. The dimension of x was about 5% larger than it should have been according to the free-electron model; the other dimensions agree with the model within the limits of the line width. All these lines are at least one order of magnitude stronger than the c_1 and c_2 lines.

Let us now imagine a rotation of the normal **n** in either the (001) or (010) plane in order to study the transition from diagrams 1 and 2 to diagrams 3 and 4 (samples $2 \to 8 \to 10 \to 3$ and $1 \to 9 \to 4$). In sample 1′, where the angle between **n** and the [001] direction is 4° we already observe a splitting of one of the x cross sections (which is not shown in diagram 1 because the split lines are incompletely resolved). With further rotation of **n** the splitting is enhanced; this is shown in diagram 2, where the dot-dash lines denote the positions of the **x** lines in sample 8. It is easily seen that the cause of line splitting in these cases is about the same as for splitting of the x line into x and c
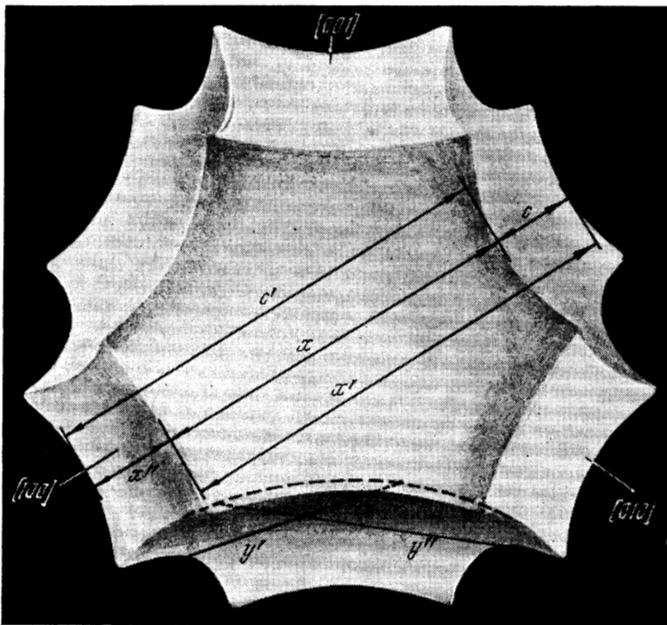
FIG. 13. View of the second zone Fermi surface from the [111] direction. Measured dimensions for **H** ∥ [0$\bar{1}$1] are indicated by arrows. Segments y′ and y″ are the locations of the intersecting plane determining the corresponding lines. The dashed curve is the geometric locus of points for which (2) is fulfilled.
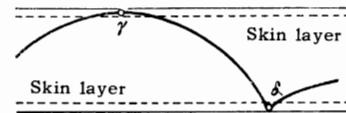

FIG. 14. Schematic drawing of a y trajectory. The corresponding points on the Fermi surface are located in a hexagonal cup (γ) and on an edge (δ). See Fig. 5 also.

when we go from the trajectory of Fig. 12b to the trajectory of Fig. 12c; when the direction of the normal becomes nonsymmetric the different hexagonal cups of the Fermi surface rotate differently with respect to the sample surface.

We consider it important that one of the split x lines tends to move into the low-field region; we here come to the portion of our data that is interpreted with the greatest difficulty - the y lines. Although we have not studied the rotation of the normal from [100] to [110] sufficiently thoroughly, there is every reason to assume that the x line moving into the low-field region becomes y′. This is shown, specifically, by the position of the y′ lines in samples 9 (diagram 4) and 10. If we assume that this transition is an established fact, the range of possible explanations of y lines immediately becomes much narrower. (We have already remarked that the y lines cannot be associated with α tubes. For about the same reasons it is difficult to imagine that these lines pertain to any other surface not included in the free-electron model.

We postulate that the y lines depend on the concavity of the hexagonal cups of the second zone surface; a part of the corresponding trajectory is represented schematically in Fig. 14. In diagram 3 the solid line γ and the outside dashed lines δ and ϵ denote, respectively, the projection of points

with $v \cdot n$ = 0 and of Fermi surface edges on the sample plane. Extremal cross sections are easily distinguished here in certain angular intervals (which coincide approximately with the intervals where y_3 and y'_3 lines exist). The straight line 1 is the trace of the extremal intersection for **H** ∥ [$\bar{1}$10] (the corresponding dimension is indicated on the diagram in the 90° direction), and the straight lines 2 and 3 are the same for a field rotated ±10° from [$\bar{1}$10].

It should be noted that in diagram 3 the upper and lower edges of the Fermi surface are projected onto a single line. This does not occur for other normals **n** (for example, in diagram 4), so that each y line should be split. This splitting was observed only in samples 6 and 10; in sample 6 the y line should have been visible along the entire tube (like c_5), but it was actually observed only at its ends. A similar explanation can be proposed for the y_5 lines (Fig. 13).

Conclusions. A twofold result has thus been derived from the investigation of the size effect in the second zone Fermi surface. First, on the basis of the free-electron model several new features of the electromagnetic field distribution within a metal were discovered; these are associated with features of the electron trajectory shapes (splitting of size effect lines for extremal helical trajectories in an inclined magnetic field[11] and the size effect at sharp bends of the electron trajectories). Secondly, measurements obtained by the size effect method lead to some conclusions concerning the shape of the second zone surface, thus improving the free-electron model.

Confirmation is apparently obtained for a result of galvanomagnetic measurements[4,5] according to which the junctions predicted by the model at W′ corners are not realized. The behavior of the a_2 and a_4 lines near a W′ corner indicates the opposite, i.e., that these corners of the surface are highly rounded. The same can be said regarding the W corners (in connection with the lines a_1 and a'_2 (see also[7]). Moreover, the existence of junctions would have led to the appearance of a number of additional lines, including those from open trajectories, but such lines were not detected experimentally.

We note that, unexpectedly, the edges of the surface remain quite sharp. This refers primarily to the edges between hexagonal cups. This is an interesting fact that requires further study.

The authors are indebted to Academician P. L. Kapitza for enabling them to work at the Institute for Physics Problems of the USSR Academy of Sciences, and to Yu. V. Sharvin and R. T. Mina for discussions of the results.

[1] A. A. Abrikosov and L. A. Fal'kovskiĭ, JETP 43, 1089 (1963), Soviet Phys. JETP 16, 769 (1963).

[2] G. N. Kamm and H. V. Bohm, Phys. Rev. 131, 111 (1963).

[3] E. P. Vol'skiĭ, JETP 46, 123 (1964), Soviet Phys. JETP 19, 89 (1964).

[4] V. G. Volotskaya, JETP 45, 49 (1963), Soviet Phys. JETP 18, 36 (1964).

[5] Yu. P. Gaĭdukov, JETP 49, 1049 (1965), this issue, p. 730.

[6] J. A. Rayne, Phys. Rev. 129, 652 (1963).

[7] P. T. Mina and M. S. Khaĭkin, JETP 48, 111 (1965), Soviet Phys. JETP 21, 75 (1965).

[8] G. B. Brandt and J. A. Rayne, Phys. Rev. 132, 1512 (1963).

[9] G. B. Brandt and J. A. Rayne, Phys. Letters 12, 87 (1964).

[10] V. F. Gantmakher, JETP 44, 811 (1963), Soviet Phys. JETP 17, 549 (1963).

[11] V. F. Gantmakher and I. P. Krylov, JETP 47, 2111 (1964), Soviet Phys. JETP 20, 1418 (1965).

[12] I. P. Krylov, JETP Pis'ma 1, No. 4, 24 (1965), JETP Letters 1, 46 (1965).

[13] V. F. Gantmakher, JETP 43, 345 (1962), Soviet Phys. 16, 247 (1963).

[14] A. B. Pippard, in The Fermi Surface, edited by W. A. Harrison and M. B. Webb, John Wiley and Sons, Inc., New York, 1960, p. 230.

[15] M. Ya. Azbel', JETP 39, 400 (1960), Soviet Phys. JETP 12, 283 (1961).

[16] É. A. Kaner, JETP 44, 1036 (1963), Soviet Phys. JETP 17, 700 (1963).

[17] B. Segall, Phys. Rev. 131, 121 (1963).